

FIRST RESULTS OF PLASMA AND NEUTRAL GAS MEASUREMENTS FROM VEGA-1/2 NEAR COMET HALLEY

K. I. Gringauz,* T. I. Gombosi,** A. P. Remizov,*
I. Apáthy,** I. Szemerey,** M. I. Verigin,*
L. I. Denchikova,* A. V. Dyachkov* E. Keppler,***
I. N. Klimenko,* A. K. Richter,*** A. J. Somogyi,**
K. Szegő,** S. Szendrő,** M. Tátrallyay,**
A. Varga** and G. A. Vladimirova*

*Space Research Institute, Profsoyuznaya 84/32, 117810 Moscow
GSP-7, U.S.S.R.

**Central Research Institute for Physics, Hungarian Academy of
Sciences, PO Box 49, H-1525 Budapest 114, Hungary

***Max-Planck-Institut für Aeronomie, D-3411 Katlenburg-
Lindau, F.R.G.

ABSTRACT

Based on the ion, electron and neutral gas observations, performed by five of the six sensors comprising the PLASMAG-1 experiment on board VEGA-1 and -2, the following results are discussed: (1) the existence of the bow shock and its location at $\approx 1.1 \times 10^6$ km for VEGA-1 inbound; (2) the existence of a cometopause and its location at $\approx 1.6 \times 10^5$ km for VEGA-2 inbound; (3) the plasma dynamical processes occurring inside the cometosheath; (4) the phenomena taking place within the cometary plasma region including mass-spectroscopy of cometary ions at distances $\approx 1.5 \times 10^4$ km; (5) the existence of keV electrons near closest approach to the nucleus; and (6) the radial dependence of the cometary neutral gas and the comparison with model calculations, yielding a mean ionization scale length of $\approx 2 \times 10^6$ km and an overall production rate of $\approx 1.3 \times 10^{30}$ molecules s^{-1} for VEGA-1 inbound. The results are also discussed in the context of the other, both remote and in-situ, observations, performed on board the VEGA- and GIOTTO-spacecraft.

INTRODUCTION

Some initial results of the first in situ plasma and neutral gas measurements near comet Halley, as obtained by the PLASMAG-1 experiment on board the spacecraft VEGA-1 and VEGA-2, have been published recently by Gringauz et al. /1/. The aim of this report is twofold: first, to extend the discussions on these earlier observations and to add some new ones, and second, to compare some of the PLASMAG-1 results with those obtained by other field and particle experiments, carried aboard the VEGA and GIOTTO spacecraft to comet Halley.

SCIENTIFIC OBJECTIVES AND INSTRUMENTATION

The PLASMAG-1 experiment had the following scientific aims: (1) to study the overall structure and the dynamics of the plasma environment near comet Halley as a function of distance from its nucleus; (2) to investigate the existence and structure of the cometary bow shock and of other cometary boundaries, if they exist; (3) to determine the chemical composition of cometary ions in the region where their velocities are small as compared to the spacecraft-comet relative speed; and (4) to measure the total neutral gas distribution along the spacecraft trajectories.

In order to meet these scientific objectives each of the PLASMAG-1 experiments comprised six different sensors /1,2,3/. Two hemispherical electrostatic analyzers for measuring the energy/charge (E/Q) spectra of ions arriving from the spacecraft-comet relative velocity direction (the Cometary Ram Analyzer CRA) and from the direction of the Sun (the Solar Direction Analyzer SDA), respectively. As the flow direction of the incoming ions may vary within $\pm 10^\circ$ and because of the three-axis stabilization of the VEGA spacecraft, electrostatic lenses were installed at the entrance slits of both analyzers in order to widen their acceptance angles without decreasing their energy resolution. The CRA had a field of view (FOV) of 14° in the ecliptic plane and of 32° in the perpendicular direction, and it detected ions in the E/Q range 15-3500 eV/Q in 120 logarithmically spaced energy intervals covering the complete energy range without any gaps. The SDA had a FOV of 30° in the ecliptic plane and of 38° in the perpendicular direction, and it recorded ions in the E/Q range 50-25000 eV/Q in 60 logarithmically spaced energy intervals. All acceptance angle data refer to the 10% level; for the same level, the energy resolution of both sensors were

$\Delta E/E = 0.055$. It should be noted that there was a gap of 45° between the FOV's of the CRA and SDA in the Sun-comet-spacecraft plane.

Electrons were measured by a cylindrical electrostatic analyzer (EA) in 30 logarithmically spaced energy intervals with $\Delta E/E = 0.075$ in the energy range 3-10000 eV. Its FOV was $7^\circ \times 7^\circ$, and it was oriented perpendicular to the ecliptic plane. The secondary electron multiplier VEU-6 served as the sensitive element in all three sensors CRA, SDA, and EA.

During the time period considered here, i.e., from 2 d before to 1 d after the encounter with the comet, the energy spectra of the ions and electrons were continuously measured every 3 min. During the closest approach, i.e., from 3 h before to 1 h after the encounter, these spectra were recorded continuously every second. During the cruise phase in interplanetary space only the SDA and EA were switched on, and 2 spectra were measured during 5 s once per every 20 min.

PLASMAG-1 also included two Faraday cups. The Solar Direction Faraday Cup (SDFC) with a FOV of $84^\circ \times 84^\circ$ measured the solar wind ion fluxes. The Ram Faraday Cup (RFC) with a FOV of $25^\circ \times 25^\circ$ had 4 periodically changed modes of operation. Two modes measured the total charged particle flux, while the other two modes provided information on the neutral particle flux from the comet by detecting the secondary electrons and ions produced by neutrals striking a metallic emitter. The sixth sensor, the Plasma Impact Detector (PID), for measuring neutral particles will not be discussed in this report.

During the encounter with comet Halley, all sensors were in operation except for the CRA and EA aboard VEGA-1.

THE COMETARY BOW SHOCK

In Fig. 1 the sequence of E/Q spectra of ions is shown, as obtained by the SDA aboard VEGA-1 from about 10 UT on March 5 to 8:20 UT on March 6, 1986, i.e., from about 1 d before to 1 h after the actual encounter with comet Halley. This sequence is complete except for a data gap between 2:50 and 3:20 UT, which is due to malfunctioning of the telemetry system. The spectra shown in Fig. 1a are typical for the normal and rather cold solar wind, as their two maxima corresponding to protons and alpha particles, respectively, are well separated. This shape of the spectrum is again observed at the beginning of Fig. 1b. Approaching the comet, however, the following changes in the ion spectra occur: (1) a few hours before reaching the data gap at least the protons are gradually decelerated, while, at the same time, their overall distribution becomes wider, i.e., their temperature increases; (2) in crossing the data gap the ion flow is suddenly deflected towards much smaller bulk velocities and, at the same time, the proton temperature is increased drastically, so that the maximum of the alpha particle distribution becomes obliterated. These latter findings are even more obvious when comparing the first spectra of Fig. 1b with those of Fig. 1c. Certainly, the spacecraft must have traversed some kind of cometary boundary. From the analogy of the present observations

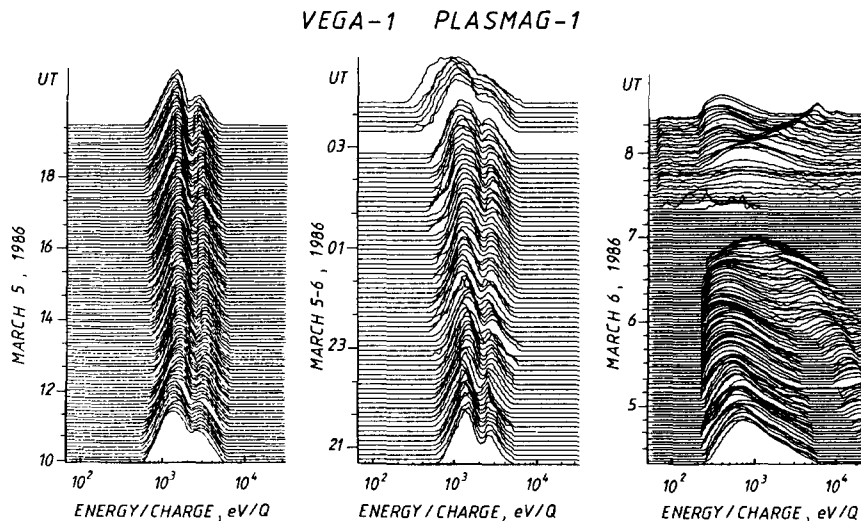


Fig. 1. Sequences of ion spectra (intensity vs. energy/charge) measured by the Solar Direction Analyzer (SDA) of the PLASMAG-1 experiment on board VEGA-1: (a) in the solar wind upstream of the comet; (b) during approach and crossing of the cometary bow shock; and (c) in the cometsheath, in the cometary plasma and back in the cometsheath region during the pre- and post-encounter of VEGA-1 with comet Halley, respectively.

with those performed at planetary bow shocks and due to the fact that these changes in the ion spectra occur rather sharply, this boundary will be called 'cometary bow shock' rather than 'cometary bow wave' - an expression which was introduced by, e.g., Jones et al. /4/ on the basis of magnetic field observations near comet Giacobini-Zinner. For the VEGA-1 inbound passage this bow shock is located at a cometocentric distance of $R_S \approx 1.1 \times 10^6$ km. For its outbound passage, however, the corresponding distances are 1.2×10^6 km or 5×10^5 km, if one takes the widening of the ion spectrum and the obliteration of the alpha particle maximum or the velocity deflection as a criterion for the bow shock crossing, respectively.

From the magnetic field measurements on board VEGA-1 Riedler et al. /5/ defined the inbound location of the bow shock at $R_S \approx 10^6$ km, while for the outbound passage a first indication of a bow shock crossing was observed at $R_S \approx 4.8 \times 10^5$ km whereas the significant drop in magnetic turbulence was seen at $R_S \approx 1.2 \times 10^6$ km. Inbound Klimov et al. /6/ identified a sharp increase in the plasma-wave intensities at 1.5 and 3.5 Hz at a distance $R_S \approx 10^6$ km. It was noted that these frequencies are characteristic for quasi-perpendicular shocks, and that the spectrum of these waves is similar to that observed upstream of the Earth's bow shock. During the GIOTTO encounter with comet Halley the bow shock was observed inbound at $R_S \approx 1.15 \times 10^6$ km in the magnetic field /7/ and at $\approx 1.13 \times 10^6$ km in the plasma data /8/, respectively. Thus, the PLASMAG-1 and the other VEGA-1 and GIOTTO observations on the inbound existence and location of the cometary bow shock are in good agreement with each other.

THE COMETOSHEATH

Downstream of the cometary bow shock both VEGA spacecraft encountered a region which was named 'cometosheath' /1/, in order to acknowledge the principal difference with respect to the physical processes occurring over this cometary region as compared to those observed in the magnetosheath of planets with strong intrinsic magnetic fields or in the ionosheath of planets with intense gravitational fields. This difference is readily seen from the ion spectra as measured by the VEGA-1 SDA (Fig. 1c) and by the VEGA-2 SDA (Fig. 2b) and CRA (Fig. 2c) over this region, as well as from the comparison of the ion spectra observed by the VEGA-1 SDA (Fig. 2a) in the undisturbed solar wind and, at the same time, by the VEGA-2 SDA (Fig. 2b) in the cometosheath region.

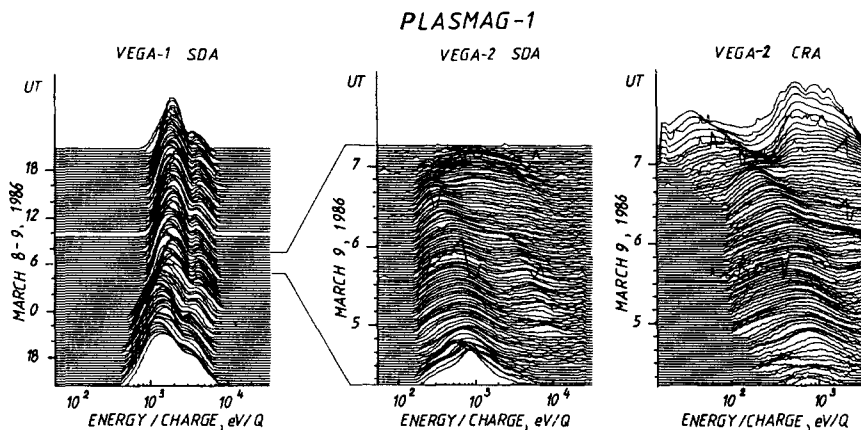


Fig. 2. Sequences of ion spectra measured (a) by the VEGA-1 SDA in the solar wind during the time of the encounter of VEGA-2; (b) by the VEGA-2 SDA downstream of the cometary bow shock and up to a cometocentric distance of $\approx 1.5 \times 10^4$ km; and (c) by the VEGA-2 Cometary Ram Analyzer (CRA) over the same distance range.

At a cometocentric distance of $R_C \approx 8 \times 10^5$ km the SDA post bow shock ion spectra are characterized by a wide, single maximum distribution of decelerated and heated solar wind ions (Figs. 1c and 2b). The proton bulk velocity is $350-400 \text{ km s}^{-1}$. Approaching the nucleus the following scenario is observed: (1) the direction of the solar wind bulk flow smoothly changes from the solar towards the ram direction, as the maximum intensities at the same energies gradually decrease (increase) in the SDA (CRA), respectively (Figs. 2b and 2c); (2) the bulk velocity of the solar wind and its temperature gradually decrease (Fig. 1c, 2b and 2c); (3) a second maximum starts to appear in the SDA spectra at higher energies (Fig. 1c), indicating that the corresponding ions initially may have had energies larger than 25 keV, which are not observable by the SDA. Certainly, these latter ions must be of cometary origin. Comparing the energies at the two peaks in the ion spectra, it is reasonable to deduce that these ions originate from the water-group (O^+ , OH^+ , H_2O^+ , H_3O^+),

which are trapped by the magnetic field and accelerated to velocities of twice the solar wind speed. Due to some not yet fully understood collective processes these cometary ions are then decelerated rather drastically, and within about 3×10^5 km these ions even start to merge with the solar wind ion population. As a result one rather broad, single peak ion distribution is observed shortly before the SDA ceases to detect any further ion flux from the solar direction, which occurs at $R_C \approx 1.6 \times 10^5$ km (Fig. 1c). After its closest approach to the comet (at 7:20 UT and $R_C = 9000$ km) VEGA-1 again starts to detect ions coming from the solar direction at 7:35 UT, and while flying outbound the scenario outlined above repeats itself just in an opposite way (Fig. 1c).

The PLASMAG-1 cometsheath observations described above have been verified by the measurements of the IIS sensor aboard GIOTTO /8/. In addition, however, the IIS observations have added a new piece of information concerning the dynamical evolution of the cometary water-group ions. Initially, these ions are observed by the IIS in a fairly narrow energy band at an energy of 32 keV, i.e., beyond the energy range of the SDA ($E_{Max} = 25$ keV). As the nucleus is approached, the energy of these ions gradually decreases along with the flow energy of the solar wind ions. Their energy remains larger than about 20 keV nearly throughout the cometsheath region. Within the cometsheath a second, yet less energetic cometary ion population starts to separate itself and to reduce its bulk speed fairly rapidly in the same way as has been observed by the VEGA-1 SDA (Fig. 1c). Although, both populations are believed to comprise water-group ions of cometary origin, their dynamical behaviour within the cometsheath region is very different. One explanation of this difference could be the following one: the more energetic implanted ions originate from neutrals being ionized directly at or near the point of observation. Their energy would then be solely determined by the local solar wind velocity, and thus these ions and the solar wind ions would undergo a deceleration in parallel. The second, less energetic population of implanted ions was originally formed much further out from the comet, i.e., far outside the point of observation. While flowing with the solar wind towards the comet these ions were then subjected to some collective, yet unknown processes, resulting in an enhanced deceleration while approaching the comet. Thus, the difference in energy between both populations will become larger as the distance to the nucleus decreases.

THE COMETOPAUSE

At about 6:45 UT or, equivalently, at $R_C \approx 1.6 \times 10^5$ km the SDA practically discontinues to detect solar wind ions coming from the solar direction (Fig. 2b). At the same time the CRA spectra (Fig. 2c) are characterized (1) by a flattening and a decrease in intensity of the solar wind ion distribution, and (2) by the appearance of a second, rather broad ion distribution at larger E/O values, which has been practically absent before. These processes, as observed by the SDA and CRA aboard VEGA-2, do not only occur simultaneously but also very abruptly. This becomes more obvious from the colour-coded representation of the SDA and CRA measurements, as displayed in Fig. 3. Here the intensities in the particle spectra, as measured by the EA (upper panel), by the CRA (middle panel), and by the SDA (lower panel) over the time period indicated at the bottom, are represented by colour (see left-hand colour table). On the vertical axis the corresponding energy and energy/charge scales are shown, respectively. From this figure it is quite obvious that between 6:43 and 6:45 UT ($R_C \approx 1.7-1.6 \times 10^5$ km) VEGA-2 has crossed a rather sharp boundary, which separates two plasma regimes of different chemical composition from each other, namely the solar wind controlled region in the 'cometsheath' from the cometary plasma region dominated by heavy cometary ions (partly observed also by the SDA). This boundary was named the 'cometopause' /9/.

Other experiments aboard VEGA-2 seem to have detected no special indications for the existence of a 'cometopause'. In the GIOTTO data, however, some kind of boundary is observed at $R_C \approx 1.35 \times 10^5$ km, behind which the magnetic field intensity suddenly starts to rise /7/, or at $R_C \approx 1.5 \times 10^5$ km, behind which the density of the heavy cometary ions starts to increase /10/, or at $R_C \approx 1.4 \times 10^5$ km, behind which the density of the electrons with energies > 10 eV suddenly decreases /11/. With respect to this latter observation this boundary was also called 'collisionopause'.

THE COMETARY PLASMA REGION

Further downstream of the 'cometopause' at about 7:00 UT the VEGA-2 CRA observations depicted in Figs. 2c or 3 indicate that there are essentially two separate ion populations present: A first one, which consists mainly of protons (see below), gives rise to the left-hand or lower distribution in the ion spectra, while the second one, which consists of cometary ions (see below), forms a rather broad, right-hand or upper distribution. As the nucleus is approached, the following changes in these two distributions are observed: (1) their maximum intensities increase gradually, however, the increase for the cometary ions occurs much faster (Fig. 3). Due to this increasing dominance of cometary ions this regime is called the 'cometary plasma region'. From the high-time resolved ion spectra depicted in Fig. 4 (time-marks correspond to 10 s each) it readily follows that this increase in the intensity of the cometary ions actually does not occur in a steady,

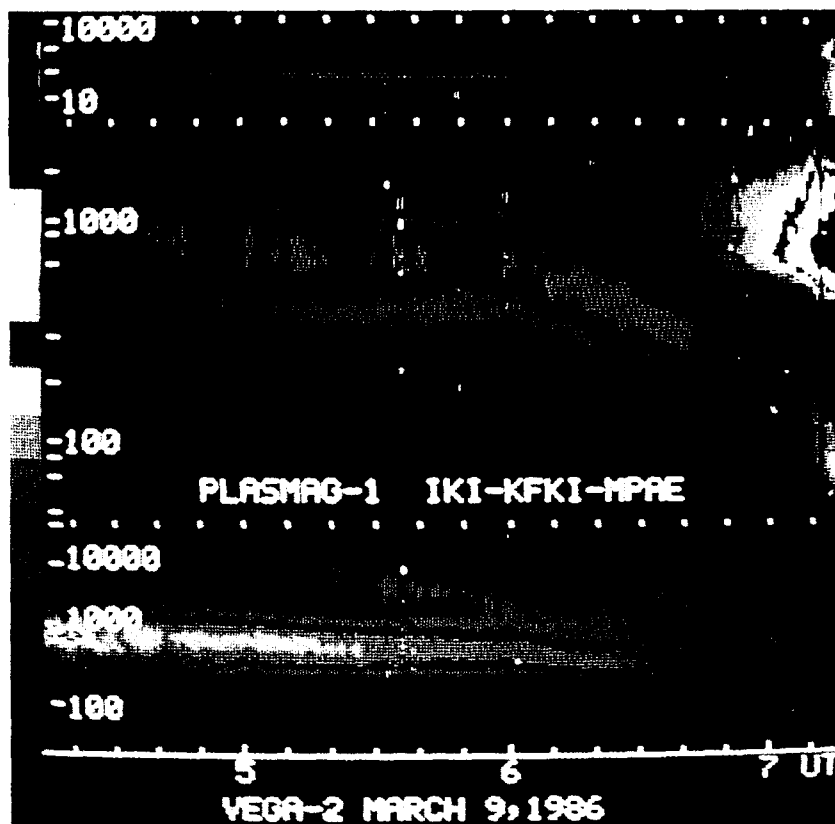


Fig. 3. Colour-coded representation of the intensities (see colour-table) vs. energy or energy/charge (vertical axis) and time (horizontal axis) of electrons measured by the Electron Analyzer (upper panel), and of ions detected by the CRA (middle panel) and SDA (lower panel), respectively. Notice the location of the 'cometopause' at $\approx 6:45$ UT or at a cometocentric distance of $\approx 1.6 \times 10^5$ km.



Fig. 4. Colour-coded representation of the intensities (see colour-table in Fig. 3) vs. energy/charge (vertical axis) and time (horizontal axis with 10 s time-marks) of cometary ions measured by the VEGA-2 CRA within the 'cometary plasma region' from 7:00 to 7:04 UT. Notice the quasi-periodical occurrence of cometary ions in lumps.

homogeneous but rather in a quasi-periodic, lumpy way. This occurrence of cometary ions in clusters at distances $R_C > 5 \times 10^4$ km is not yet understood. The typical scale-length of this structure along the spacecraft trajectory is about 800 km.

(2) the proton population decelerates rather rapidly. Near closest approach to the nucleus its maximum intensity is located at about 30 eV/Q (Fig. 5a). In turn, this would be exactly the E/Q value of a proton having a velocity equal to the spacecraft velocity of 76.8 km s^{-1} . This observation clearly proves that it is the protons (presumably of cometary origin) that mainly contributed to the left-hand distribution of the ion spectra in the 'cometary plasma region', and that the spacecraft velocity has exceeded in this part of this regime both the thermal and the bulk velocities of the ions. In contrast to the protons the heavier ions are not decelerated within the 'cometary plasma region', indicating that this regime is dominated by stagnating cometary ions. This, in turn, might explain the formation of a distinct boundary, the 'cometopause', rather than of a soft transition zone between the 'cometosheath' and the 'cometary plasma region'.

(3) both distributions become narrower, indicating that the temperature of both populations gradually decreases. The effect on the overall cometary ion distribution is that it starts to break-up into several separate sub-distributions at a distance of $R_C \approx 5 \times 10^4$ km. Near closest approach, i.e., at $R_C < 1.5 \times 10^4$ km, when both the thermal and the bulk velocities of the ions become small compared to the spacecraft velocity, the maxima of these various sub-distributions organize themselves along certain fixed E/Q values. This situation is depicted in Figs. 5a and 5b, where the count rates in the E/Q channels are plotted on a logarithmic and on a linear vertical scale, respectively. As the velocity at which the cometary ions are detected by the CRA is more or less the spacecraft velocity, the E/Q spectra can be transformed into mass/charge (M/Q) spectra. The position of some characteristic M/Q values are marked by arrows in Figs. 5a and 5b. Finally, this observation clearly proves that the ions, which contributed to the right-hand, initially broad distribution of the ion spectra in the 'cometary plasma region' are of cometary rather than of solar wind origin.

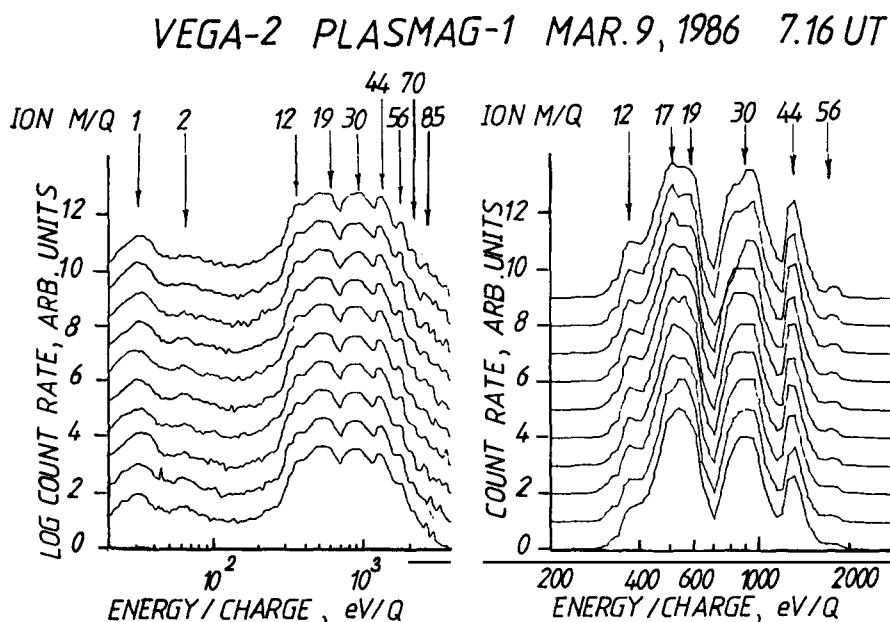


Fig. 5. Sequences of cometary ion spectra, averaged over 4 s, as measured by the VEGA-2 CRA at a cometocentric distance of $\approx 1.5 \times 10^4$ km. The intensities are plotted (a) on a logarithmic, and (b) on a linear vertical scale, respectively. As the ion thermal- and bulk speeds are small compared to the spacecraft ram velocity, the energy/charge scale can be transformed into a mass/charge (M/Q) scale. Some characteristic M/Q values are indicated at the top.

On the basis of Figs. 5a and 5b ions, such as H^+ , C^+ , CO_2^+ and Fe^+ , can be identified with some confidence. The structured peak at $14 < M/Q < 20$ most probably originates from H_2O parent molecules, with major contributions of O^+ , OH^+ and H_3O^+ ions. The peak at $24 < M/Q < 34$ may have formed from CO/CO_2 parent molecules or of molecules bearing N or S, such as CO^+ , N_2^+ , H_2CO^+ , HCO^+ , CN^+ , HCN^+ or O_2^+ , or from atomic ions, such as Mg^+ , Al^+ , Si^+ , P^+ or S^+ . Several smaller peaks at $M/Q \approx 2, 8, 70$ and 85 could be due to H_2^+ and O^{++} and to some heavier organic molecules or ion-water clusters. It should be stressed that the count

rates depicted in Figs. 5a and 5b do not represent the actual densities, as with respect to some main peaks the corresponding counting rates occur in the nonlinear regime of the channeltron, so that the proper calibration data have to be taken into account for a conversion into densities.

From their GIOTTO measurements Balsiger *et al.* /10/ determined the velocity of the main cometary ions relative to the comet to be about 3 km s^{-1} within $R_C \approx 2.5 \times 10^4 \text{ km}$ and about 1 km s^{-1} within $R_C \approx 1.5 \times 10^4 \text{ km}$. Moreover, the various M/Q groups identified by the PLASMAG-1 experiment are in agreement with the ion and neutral mass spectrometer observations performed aboard GIOTTO /10,12,13/.

COMETARY ELECTRONS

From the PLASMAG-1 EA measurements aboard VEGA-2 we find that the electron spectrum does not change significantly throughout the 'cometosheath region' and while crossing the 'cometopause' (Fig. 3, top panel). However, at about 7:00 UT, when the two ion populations in the CRA spectra start to separate, electrons are detected also at higher energies. These electrons then form a well defined peak at a few keV at a distance $R_C \approx 1.5 \times 10^4 \text{ km}$. This situation is shown in Fig. 6, presenting two typical electron spectra: The lower one observed in the solar wind and the upper one measured at the distance $R_C \approx 1.5 \times 10^4 \text{ km}$. The main difference between these spectra is the appearance of the energetic cometary electron component, which could serve as an additional source of ionization of cometary neutrals.

It is worth noticing that these energetic cometary electrons seem to be present in a region (1) over which the magnetic field direction rapidly rotates, i.e., within the region of ordinary magnetic field-line draping /5/, and (2) where sudden enhancements in the intensities of low-energy ions are observed /14/ in case of the VEGA-1 fly-by. It should also be mentioned that these electrons have not been observed by GIOTTO /11/.

DISTRIBUTION OF COMETARY NEUTRAL GAS

As outlined in chapter one, a subset of the PLASMAG-1 Ram Faraday Cup (RFC) measurements can be used to determine the integrated flux of the overall cometary 'neutral gas' arriving from the spacecraft-comet relative velocity direction. From a distance $R_C \approx 3 \times 10^6 \text{ km}$ onwards

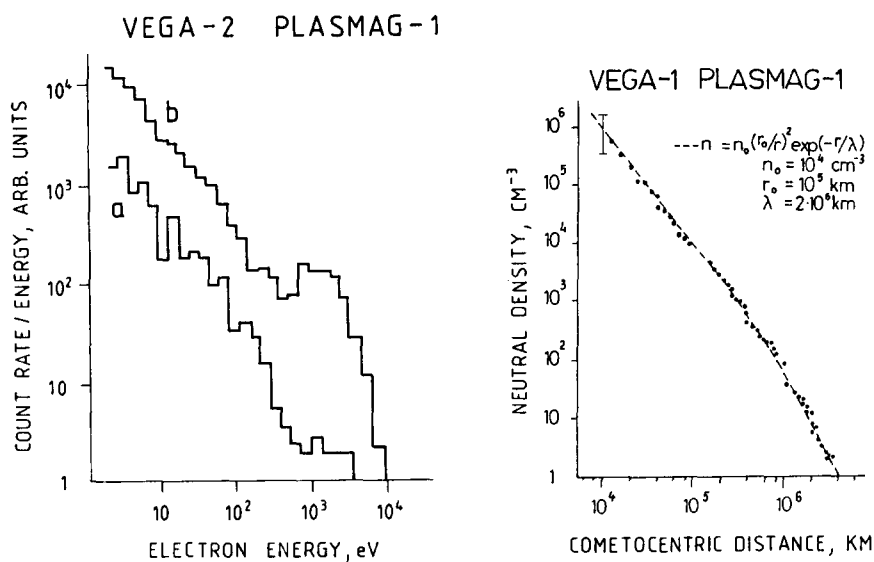


Fig. 6. Two electron spectra, as measured by the VEGA-2 Electron Analyzer in the solar wind (curve a) and near closest approach to the cometary nucleus at $\approx 1.5 \times 10^4 \text{ km}$ (curve b), respectively. Notice the occurrence of keV electrons close to the nucleus.

Fig. 7. Radial profile of the overall 'neutral gas' density, as measured inbound by the VEGA-1 Ram Faraday Cup. Comparison with the distribution predicted by theory (dotted line) yields an ionization scale length of $\approx 2 \times 10^6 \text{ km}$ and an overall production rate of $\approx 1.3 \times 10^{30} \text{ molecules s}^{-1}$.

the yield of secondary electrons originating from the impact of 'neutral particles' increased sharply, and it reached saturation at about $R_c \approx 10^5$ km. Further downstream the current of secondary ions was used to determine the neutral gas flux. In order to evaluate the corresponding densities, a yield of ≈ 0.3 and of $\approx 5 \times 10^{-4}$ for secondary electrons and ions at the emitter-plate is considered, respectively. In Fig. 7 the cometary neutral gas density, as obtained from the VEGA-1 RFC inbound measurements, are shown as a function of cometocentric distance. These measurements are plotted as dots, and a typical error-bar is included in the left-hand upper corner. For the density $n(r)$ of cometary neutrals, model calculations /15/ provide a cometocentric radial dependence $n(r) = n_0(r_0/r)^2 \exp(-r/\lambda)$. From the dotted line plotted through the data points of Fig. 7 one can estimate from its left-hand part ($r < 10^5$ km) an initial neutral gas density of $n_0 = 10^4 \text{ cm}^{-3}$, and from its right-hand part ($r > 4 \times 10^5$ km) an ionization scale length of $\lambda = 2 \times 10^6$ km. Assuming a spherically symmetric expansion, the total gas production rate is $\approx 1.3 \times 10^{30}$ particles s^{-1} within an accuracy of a factor of 2 to 3.

From the neutral gas experiment aboard VEGA-1 a radial dependence of $r^{-2.3}$ for $r < 4 \times 10^4$ km is found inbound for neutral particles of the mass 32 amu /16/. From the three-channel spectrometer aboard VEGA-2 the production rates for H_2O and OH were estimated from the visible and near-infrared spectral observations to be $\approx 4 \times 10^{29}$ and 1.7×10^{30} molecules s^{-1} , respectively /17/. From measurements of the near-ultraviolet and visible channel an OH production rate of $\approx 9 \times 10^{29}$ molecules s^{-1} was determined /18/. Finally, a preliminary estimate of the overall production rate of $\approx 6.9 \times 10^{29}$ molecules s^{-1} was provided by Krankowsky et al. /12/ from their neutral mass spectrometer observations aboard GIOTTO. Thus, by comparison with these results obtained independently, it is fair to state that the PLASMAG-1 RFC measurements provide a rather reliable description of the 'neutral gas' environment of comet Halley.

GENERAL OVERVIEW

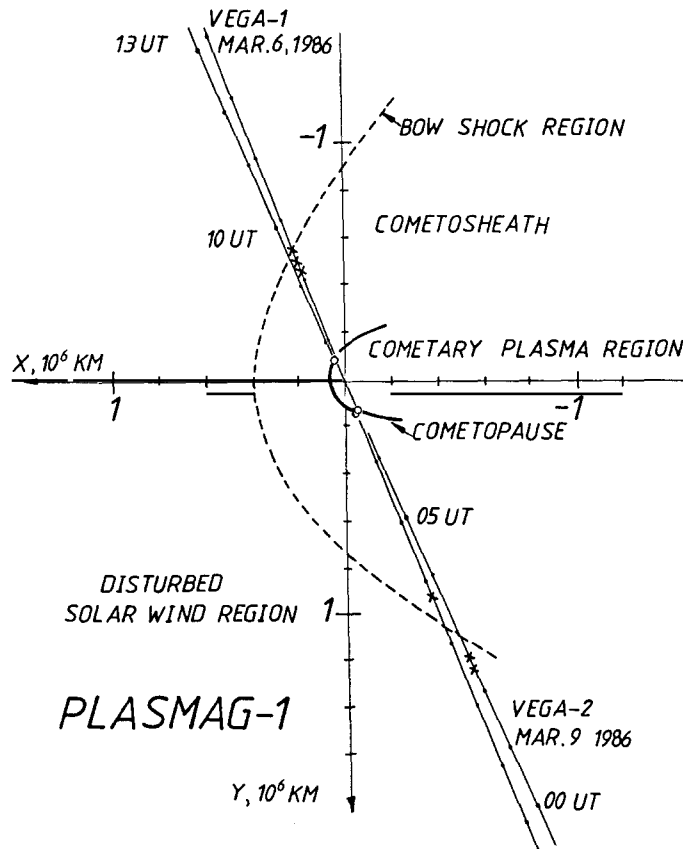


Fig. 8. General overview on the in- and outbound locations of the 'bow shock' and of the 'cometopause' as well as of the 'cometosheath' and of the 'cometary plasma region', as identified from the PLASMAG-1 plasma observations on board VEGA-1 and -2 during their encounter with comet Halley.

REFERENCES

1. K.I. Gringauz, T.I. Gombosi, A.P. Remizov, I. Apáthy, I. Szemerey, M.I. Verigin, L.I. Denchikova, A.V. Dyachkov, E. Keppler, I.N. Klimenko, A.K. Richter, A.J. Somogyi, K. Szegő, S. Szendrő, M. Tátrallyay, A. Varga, and G.A. Vladimirova, Nature 321, 282 (1986).
2. K.I. Gringauz, I.N. Klimenko, A.P. Remizov, M.I. Verigin, G.A. Vladimirova, I. Apáthy, K. Szegő, I. Szemerey, S. Szendrő, M. Tátrallyay, E. Keppler, and A.K. Richter, in: Field-, Particle- and Wave Experiments on Cometary Missions, eds. K. Schwingenschuh and W. Riedler, IWF-Preprint 8601, Graz 1986, p. 157.
3. K.I. Gringauz, I. Apáthy, L.I. Denchikova, T.I. Gombosi, E. Keppler, I.N. Klimenko, A.P. Remizov, A.K. Richter, G.A. Skuridin, A.J. Somogyi, L. Szabó, I. Szemerey, S. Szendrő, M.I. Verigin, G.A. Vladimirova, and G.I. Volkov, in: Cometary Exploration III, ed. T.I. Gombosi, Central Research Institute for Physics, Budapest 1982, p. 333.
4. D.E. Jones, E.J. Smith, J.A. Slavin, B.T. Tsurutani, G.L. Siscoe, and D.A. Mendis, Geophys. Res. Letters 13, 243 (1986).
5. W. Riedler, K. Schwingenschuh, Ye.G. Yeroshenko, V.A. Styashkin, and C.T. Russell, Nature 321, 288 (1986).
6. S. Klimov, S. Savin, Ya. Aleksevich, G. Avanesova, V. Balebanov, M. Balikhin, A. Galeev, B. Gribov, M. Nozdrachev, V. Smirnov, A. Sokolov, O. Vaisberg, P. Oberc, Z. Krawczyk, S. Grzedzielski, J. Juchniewicz, K. Nowak, D. Orłowski, B. Parfianovich, D. Wozniak, Z. Zbyszynski, Ya. Voita, and P. Triska, Nature 321, 292 (1986).
7. F.M. Neubauer, K.H. Glassmeier, M. Pohl, J. Raeder, M.H. Acuna, L.F. Burlaga, N.F. Ness, G. Musmann, F. Mariani, M.K. Wallis, E. Ungstrup, and H.U. Schmidt, Nature 321, 352 (1986).
8. A. Johnstone, A. Coates, S. Kellock, B. Wilken, K. Jockers, H. Rosenbauer, W. Stüdemann, W. Weiss, V. Formisano, E. Amata, R. Cerulli-Irelli, M. Dobrowolny, R. Terenzi, A. Egidi, H. Borg, B. Hultqvist, J. Winningham, C. Gurgiolo, D. Bryant, T. Edwards, W. Feldman, M. Thomson, M.K. Wallis, L. Biermann, H. Schmidt, R. Lüst, G. Haerendel, and G. Paschmann, Nature 321, 344 (1986).
9. K.I. Gringauz *et al.*, Geophys. Res. Letters, in press (1986).
10. H. Balsiger, K. Altwegg, F. Bühler, J. Geiss, A.G. Ghielmetti, B.E. Goldstein, R. Goldstein, W.T. Huntress, W.-H. Ip, A.J. Lazarus, A. Meier, M. Neugebauer, U. Rettenmund, H. Rosenbauer, R. Schwenn, R.D. Sharp, E.G. Shelley, E. Ungstrup, and D.T. Young, Nature, 321, 330 (1986).
11. H. Rème, J.A. Sauvaud, C. d'Uston, F. Cotin, A. Cros, K.A. Anderson, C.W. Carlson, D.W. Curtis, R.P. Lin, D.A. Mendis, A. Korth, and A.K. Richter, Nature 321, 349 (1986).
12. D. Krankowsky, P. Lämmerzahl, I. Herrwerth, J. Woveries, P. Eberhardt, U. Dolder, U. Herrmann, W. Schulte, J.J. Berthelier, J.M. Illiano, R.R. Hodges, and J.H. Hoffman, Nature 321, 326 (1986).
13. A. Korth, A.K. Richter, A. Loidl, K.A. Anderson, C.W. Carlson, D.W. Curtis, R.P. Lin, H. Rème, J.A. Sauvaud, C. d'Uston, F. Cotin, A. Cros, and D.A. Mendis, Nature 321, 335 (1986).
14. A.J. Somogyi, K.I. Gringauz, K. Szegő, L. Szabó, Gy. Kozma, A.P. Remizov, J. Erő Jr., I.N. Klimenko, I. T.-Szűcs, M.I. Verigin, J. Windberg, T.E. Cravens, A. Dyachkov, G. Erdos, M. Faragó, T.I. Gombosi, K. Kecskeméty, E. Keppler, T. Kovács Jr., A. Kondor, Y.I. Logachev, L. Lohonyai, R. Marsden, R. Redl, A.K. Richter, V.G. Stolpovskii, J. Szabó, I. Szentpétery, A. Szepesváry, M. Tátrallyay, A. Varga, G.A. Vladimirova, K.P. Wenzel, and A. Zarándy, Nature, 321, 285 (1986).
15. L. Haser, Bull. Acad. r. Belg. Cl. Sci 43, 740 (1957).
16. E. Keppler, V.V. Afonin, C.C. Curtis, A.V. Dyachkov, J. Erő Jr., C.Y. Fan, K.C. Hsieh, D.M. Hunten, W.-H. Ip, A.K. Richter, A.J. Somogyi, and G. Umlauf, Nature 321, 273 (1986).
17. V.A. Krasnopolsky, M. Gogoshev, G. Moreels, V.I. Moroz, A.A. Krysko, Ts. Gogosheva, K. Palazov, S. Sargoichev, J. Clairemidi, M. Vincent, J.L. Bertaux, J.E. Blamont, V.S. Troshin, and B. Valnicec, Nature 321, 269 (1986).
18. G. Moreels, M. Gogoshev, V.A. Krasnopolsky, J. Clairemidi, M. Vincent, J.P. Parisot, J.L. Bertaux, J.E. Blamont, M.C. Festou, Ts. Gogosheva, S. Sargoichev, K. Palasov, V.I. Moroz, A.A. Krysko, and V. Vanysek, Nature 321, 271 (1986).